Regular article

Microstructure and thermoelectric properties of Bi-Sb-Te bulk materials fabricated from rapidly solidified powders

Zhi-Lei Wang [a], Takahiro Akao [b], Tetsuhiko Onda [a], Zhong-Chun Chen [a],*

[a] Department of Mechanical and Aerospace Engineering, Graduate School of Engineering, Tottori University, Koyama-minami 4-101, Tottori 680-8552, Japan
[b] Department of Mechanical Engineering, National Institute of Technology, Fukushima College, Nagao 30, Taira Kamiarakawa, Iwaki 970-8034, Japan

ABSTRACT

A rapid solidification and spark plasma sintering technique was applied to fabricate Bi-Sb-Te bulk thermoelectric materials. Although the grain boundaries in sintered samples were primarily composed of large-angle boundaries, a large fraction of small-angle boundaries was found at a high sintering temperature. As the sintering temperature increased, the Seebeck coefficient was almost unchanged while the electrical resistivity gradually decreased. The thermal conductivity gently increased till 420 °C, and then abruptly increased. As a result, the largest ZT value of 1.1 was achieved for the sample sintered at 400 °C, which is increased by 44.7% compared with that prepared from mechanically alloyed powders.

© 2017 Acta Materialia Inc. Published by Elsevier Ltd. All rights reserved.

Thermoelectric conversion, as one of the most promising technologies to solve the impending issues of energy shortage and environmental pollution, has attracted much attention in recent years [1–4]. The conversion efficiency of a thermoelectric device highly depends on materials' dimensionless figure of merit (ZT) defined as $ZT = \alpha^2 T/(\rho\kappa)$, where α, ρ, κ, and T are the Seebeck coefficient, electrical resistivity, thermal conductivity, and absolute temperature, respectively.

Bi_2Te_3-based compounds, known as the most effective thermoelectric materials near room temperature, have been widely used in various electronic cooling devices [5], owing to fast and precise control of temperature and free of noise during the operations. In our previous work [6,7], from the viewpoints of grain refinement and preferred orientation, a combination of mechanical alloying (MA) and hot extrusion was used to fabricate Bi_2Te_3-based bulk materials. The extruded samples exhibited fine-grained microstructure and highly oriented texture, which are beneficial to the improvement in both thermoelectric and mechanical properties. However, it is difficult to obtain large amounts of alloy powders through the MA process. In the present work, a rapid solidification (RS) method was proposed to prepare Bi_2Te_3-based alloy powders, followed by consolidation through spark plasma sintering (SPS) technique. The objective of this study was to investigate the microstructure and thermoelectric properties of Bi-Sb-Te bulk materials fabricated from rapidly solidified powders.

High purity Bi, Sb, and Te (>99.99% purity) powders were used as the starting materials. The master ingots with a nominal composition of $Bi_{0.4}Sb_{1.6}Te_3$ were prepared using a high-frequency melting furnace. The ingots were melted again in a quartz tube through induction heating under vacuum, followed by rapid solidification in a gas atomization equipment (VF-RQP200) using Ar gas with an injection pressure of 5 MPa. Subsequently, the RSed powders were consolidated by SPS in a temperature range of 340–450 °C with a holding time of 5 min under an axial compressive stress of 50 MPa.

The density of the samples was determined by the Archimedes method. Phase identification was performed by X-ray diffraction (XRD) with Cu Kα radiation. The powder morphology was observed by scanning electron microscopy (SEM). Compositional analyses were conducted by electron probe micro-analyzer (EPMA) and energy dispersive X-ray spectroscopy (EDS). Orientation imaging microscopy (OIM) analysis was performed using an SEM equipped with an electron backscattered diffraction (EBSD) system (JEOL-7001FA) at a field emission voltage of 15 kV and a scan step of 0.2 μm. Inverse pole figure (IPF) and grain-boundary maps were obtained from analyses of the EBSD data by the software TSL-OIM analysis 6.2. In order to obtain high quality image, cleanup procedures were applied with a tolerance angle of 5° and a minimum grain size of 5 pixels. It should be noted that the effect of cleanup on orientation determination can be ignored when the scan step is quite smaller than the grain size [8,9]. All the thermoelectric properties were measured at 300 K. The electronic transport properties were evaluated by a Hall effect measurement system (Resi Test 8300, TOYO Corp.). The Seebeck coefficient (α) and electrical resistivity (ρ) of the samples were simultaneously measured by static DC method and four-probe method, respectively, using a thermoelectric property test apparatus (ZEM-3, ULVAC-RIKO). The thermal conductivity (κ)

was measured by laser flash method (LFA457 Micro Flash, NETZSCH). The dimensionless figure of merit of the samples was calculated by the equation of $ZT = \alpha^2 T / (\rho \kappa)$. In addition, the mechanical properties at room temperature were evaluated by the Vickers hardness test at a load of 1.96 N (HMV-2000, Shimadzu).

The SEM observations indicated that the RSed powders exhibited a spherical morphology with particle sizes of <10 μm, as shown in Fig. 1(a). The XRD pattern of the RSed powders (Fig. 1(b)) was identified as $Bi_{0.4}Sb_{1.6}Te_3$ single phase, and all the diffraction peaks were in a good agreement with the standard diffraction data (JCPDS-ICDD: 01-072-1836).

When the RSed powders were sintered by SPS in the temperature range of 340–450 °C, all the samples had high relative density values of >99% with $Bi_{0.4}Sb_{1.6}Te_3$ single phase. Figs. 2(a)–(c) show the IPF maps of the samples sintered at different temperatures, revealing the morphologies, sizes, and orientations of the grains in the SPSed samples. A featured microstructure with irregular polygon-shaped grains and random crystal orientations was observed. As the sintering temperature increased, grain growth occurred, although it appears that the grain growth is not evident from 400 °C to 450 °C. The average grain sizes were measured to be 1.19 μm, 1.62 μm, and 1.87 μm with average standard deviations of 0.6 μm, 1.02 μm, and 0.84 μm for the samples sintered at 340 °C, 400 °C, and 450 °C, respectively. Here, it is worth noting that the grain sizes were averaged from different measurement areas for each sample. In addition, large amount of twin boundaries were observed in all the samples, where the twin boundaries expressed by dark lines in Figs. 2(a)–(c) exhibited linear feature and most of them traversed the grains. As is well known, twinning occurs easily in rhombohedral Bi_2Te_3-based compounds, although basal plane slip is dominant during plastic deformation at elevated temperatures. Twin formation depends to a large extent on deformation method, strain, temperature, and so on, a more detailed discussion on twin features in Bi_2Te_3-based compounds will be given elsewhere.

In order to obtain detailed microstructural information, the grain boundary characteristics were further examined and the boundary maps corresponding to the IPF maps in Figs. 2(a)–(c) are shown in Figs. 2(d)–(f). It has been reported that EBSD patterns with a confidence index of >0.1 can correctly index an orientation at 95% [10]. In the present work, the average confidence indexes of the patterns were >0.63, which led to >99.9% of the patterns being indexed correctly, indicating high reliability [11]. The misorientation angle was divided into three levels: <5°, 5–15°, and >15° which were drawn by red, green, and blue lines, respectively. It is clear that the grain boundaries are primarily composed of large-angle boundaries (blue lines) with misorientation angles of >15°. Moreover, the fractions of small-angle boundaries (<15°), expressed by grain boundary length, were quantified as 22.9%, 11.1%, and 51.2% for the samples sintered at 340 °C, 400 °C, and 450 °C, respectively. These results indicate that the small-angle boundaries including

subgrain boundaries with angles <5° decreased with increasing sintering temperature from 340 °C to 400 °C, and then increased significantly at 450 °C. The reduction of small-angle boundaries from 340 °C to 400 °C is believed to be attributed to dynamic recrystallization and grain growth, whereas the increase at 450 °C may be associated with the formation of a Te-rich phase, which can inhibit the movement of dislocations through pinning effect and result in more small-angle boundaries. The Te-rich phase with different sizes due to evaporation of Te and eutectic reaction has been confirmed by microstructural observations and compositional analyses for the sample SPSed at 450 °C (refer to Fig. S1 in Supplementary materials). The Te-rich phase was also observed in hot-extruded samples from MAed powder and the details on formation mechanisms of the Te-rich phase have been clarified in our previous work [12]. Moreover, the Te-rich phase may be also one of the reasons for slight grain growth from 400 °C to 450 °C (Figs. 2(b) and (c)) due to inhibition of boundary migration as we have demonstrated in Ref. [12].

Fig. 3(a) shows the sintering temperature dependences of carrier concentration and Hall mobility of the SPSed samples. As the sintering temperature increased, the variation of carrier concentration was not remarkable, while the mobility slightly increased. It is well known that electronic transport properties are extremely sensitive to atomic-scale lattice defects, such as vacancies and antisite defects [13–18]. In our previous work [7], we found an increased tendency of carrier concentration with increasing the processing temperature for n-type Bi-Te-Se materials fabricated by MA/hot-extrusion technique due to sublimation of Te. Liu et al. [19] have reported that, during mechanical deformation process, the sublimation of each Te results in formation of one donor-like Te vacancy $[V_{Te}]$ with two free electrons that directly lead to increase in carrier concentration for n-type materials. As for p-type Bi-Sb-Te materials, the acceptor-like antisite defects $[Bi_{Te}]$ or $[Sb_{Te}]$ are the dominant defects, where one antisite defect contributes one hole as the carrier for p-type materials. Therefore, the independence of carrier concentration on sintering temperature in this work implies that there is no evident difference in density of antisite defects in the SPSed samples, which is attributed to the lower strain process of RS/SPS compared with MA/hot-extrusion process. The gradual increase in the mobility must be associated with the grain growth that results in decrease of carrier scattering at grain boundaries.

As is well known, the Seebeck coefficient and electrical resistivity highly depend on electronic transport properties [19]. The relationship between the Seebeck coefficient and carrier concentration (n) can be given by $\alpha \approx \gamma - \ln n$, where γ is the scattering factor. The electrical resistivity can be expressed as $\rho = 1/ne\mu$, where e and μ are the electron charge and carrier mobility, respectively. Consequently, the small change of the Seebeck coefficient and slight decrease of electrical resistivity with increasing sintering temperature (Fig. 3(b)) result from the related carrier concentration and mobility.
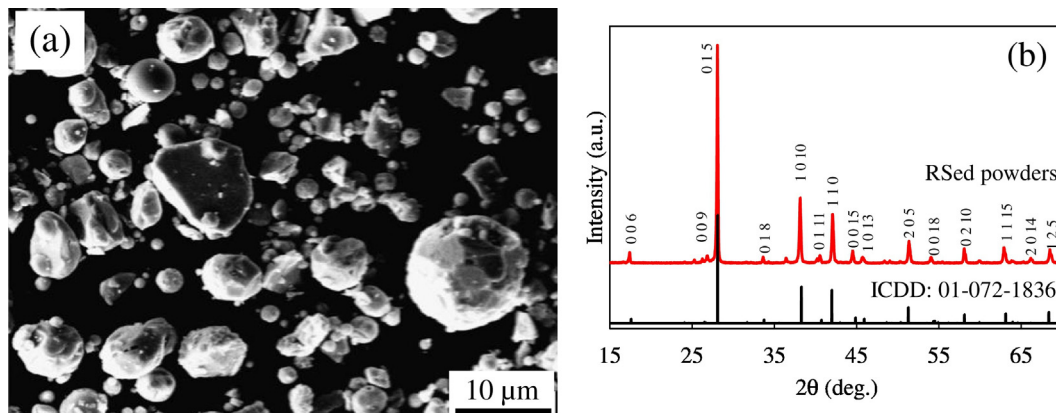

Fig. 1. (a) SEM image and (b) XRD pattern of the RSed powders.